





Article

Diatoms Dominate and Alter Marine Food-Webs When CO₂ Rises

Ben P. Harvey ^{1,*}, Sylvain Agostini ¹, Koetsu Kon ¹, Shigeki Wada ¹ and Jason M. Hall-Spencer ^{1,2}

¹ Shimoda Marine Research Center, University of Tsukuba, 5-10-1 Shimoda, Shizuoka 415-0025, Japan; agostini.sylvain@shimoda.tsukuba.ac.jp (S.A.); kon@shimoda.tsukuba.ac.jp (K.K.); swadasbm@shimoda.tsukuba.ac.jp (S.W.); jhall-spencer@plymouth.ac.uk (J.M.H.-S.)

² Marine Biology and Ecology Research Centre, University of Plymouth, PL4 8AA Plymouth, UK

* Correspondence: ben.harvey@shimoda.tsukuba.ac.jp; Tel.: +81-0558-22-6697

Received: 31 October 2019; Accepted: 9 December 2019; Published: 16 December 2019



Abstract: Diatoms are so important in ocean food-webs that any human induced changes in their abundance could have major effects on the ecology of our seas. The large chain-forming diatom *Biddulphia biddulphiana* greatly increases in abundance as $p\text{CO}_2$ increases along natural seawater CO₂ gradients in the north Pacific Ocean. In areas with reference levels of $p\text{CO}_2$, it was hard to find, but as seawater carbon dioxide levels rose, it replaced seaweeds and became the main habitat-forming species on the seabed. This diatom algal turf supported a marine invertebrate community that was much less diverse and completely differed from the benthic communities found at present-day levels of $p\text{CO}_2$. Seawater CO₂ enrichment stimulated the growth and photosynthetic efficiency of benthic diatoms, but reduced the abundance of calcified grazers such as gastropods and sea urchins. These observations suggest that ocean acidification will shift photic zone community composition so that coastal food-web structure and ecosystem function are homogenised, simplified, and more strongly affected by seasonal algal blooms.

Keywords: ocean acidification; benthic diatoms; ecological shift; CO₂ fertilisation; turf algae; habitat-forming; algal blooms; marine food-webs

1. Introduction

Diatoms are dominant marine primary producers, accounting for ~40% of ocean primary production [1]. Ocean acidification, the alteration of carbonate chemistry due to increased anthropogenic carbon dioxide, has negative impacts on many marine calcifying organisms [2], but the possible effects of this rapid change in surface ocean chemistry is still intriguing world experts. There is a growing consensus on how ocean acidification will affect marine phytoplankton [3,4]. Research into the response of diatoms to ocean acidification has mostly focussed on their growth, productivity, and community composition by using mesocosms or flask culture experiments [5], with predominantly positive effects observed. Projections of the effects of ocean acidification on diatoms suggest that increased availability of CO₂ as a substrate for photosynthesis will benefit these algae where sufficient nutrients are available [6], and that these algae may indirectly benefit through reduced grazing pressure [7]. Changes in the ecological balance of life in our world ocean due to ocean acidification is a key focus of current research as it underpins the ‘blue economy’ [8].

Diatoms are strong competitors for ocean resources when sufficient light and nutrients are present; they often dominate early stages of phytoplankton community succession in coastal ecosystems [9]. Under present-day conditions, large diatoms are often restricted by diffusion gradients as they have lower surface-to-volume ratios than smaller species [10]. In incubation experiments, large centric

diatom species benefit from CO₂ enrichment and outcompete smaller diatoms [11,12]. A shift to larger diatoms may increase the trophic transfer of energy to marine animals by shortening food chains [13], and promote production in higher trophic levels. Carbon dioxide-driven shifts towards larger diatoms has been observed in ocean acidification experiments using natural communities [7,11,12,14–17], suggesting that larger diatoms may become favoured in the future [5].

Experiments using natural communities of marine organisms are useful when projecting the impacts of ocean acidification as these help assess cascading effects through trophic levels that can only be assessed when interactions and competition among species are considered [18]. Studies investigating the effects of ocean acidification on natural diatom communities have mostly focussed on plankton (review: [5]), typically performed using closed containers [19]. In recent years, alternative approaches have increasingly been used including in situ and long-term mesocosm experiments (e.g., [16,20]) and the use of natural gradients in *p*CO₂. Volcanic seeps can reveal the long-term ecological responses of communities to acidification, while still retaining natural pH variability and intact ecological interactions. Observations along gradients of carbonate chemistry have revealed both winners and losers in acidified conditions [21–23]. For diatoms, CO₂ seep research on planktonic species is lacking, since pelagic communities are advected with currents. However, studies at CO₂ seeps have found increases in the photosynthetic standing crop of both epilithic biofilms and microphytobenthic assemblages [24,25].

Here, we assess the effect of ocean acidification on diatoms and food-webs. In the context of ecosystem services on which our society relies, it is important to understand how ocean acidification will affect the marine ecosystem structure and function. In the present study, the diatom *Biddulphia biddulphiana* (J.E. Smith) Boyer became more abundant as CO₂ levels increased with increasing proximity to a volcanic seep, and at higher levels of dissolved carbon dioxide it was the main habitat-forming species. We investigated how ocean acidification influenced the abundance, photophysiology, and habitat-provisioning of this large diatom.

2. Materials and Methods

2.1. Study Site, Carbonate Chemistry, and Nutrients

We assessed the response of the diatom *Biddulphia biddulphiana* along a natural gradient of *p*CO₂ at a volcanic seep off Shikine Island, Japan (34°19'9" N, 139°12'18" E), which we surveyed seasonally through scuba diving from 2015–2018 [22,26]. Shallow sublittoral rocky substrata were spatially dominated by a mix of canopy-forming macroalgae and zooxanthellate scleractinian corals at our reference site and all around this island, except where *p*CO₂ was higher due to seeps. In these high *p*CO₂ areas, there were algal mats previously described as 'turf algae' [22]. We used five sites along the *p*CO₂ gradient: 'Reference' (mean *p*CO₂: 410 ± 73), which was outside the influence of the CO₂ seep; 'RCP 2.6' (mean *p*CO₂: 493 ± 158); 'RCP 4.5' (mean *p*CO₂: 765 ± 159); 'RCP 6.0' (mean *p*CO₂: 971 ± 258); and '>RCP 8.5' (mean *p*CO₂: 1803 ± 1287, Table 1). The sites were termed 'RCP 2.6', 'RCP 4.5', and 'RCP 6.0' in reference to their equivalent Intergovernmental Panel on Climate Change Representative Concentration Pathway (RCP) scenarios [27]. Our >RCP 8.5 site was used to assess the abundance and physiology of diatoms to ocean acidification beyond predicted levels due to human CO₂ emissions. The areas used in this study had the same temperature, dissolved oxygen, total alkalinity, and depth [22,28].

Table 1. Carbonate chemistry of the reference, RCP 2.6, RCP 4.5, RCP 6.0, and >RCP 8.5 sites at Shikine Island, Japan.

Station	pH _T	Temp (°C)	Salinity (psu)	A _T (μmol kg ⁻¹)	pCO ₂ (μatm)	DIC (μmol kg ⁻¹)	HCO ₃ ⁻ (μmol kg ⁻¹)	CO ₃ ²⁻ (μmol kg ⁻¹)	Ωcalcite	Ωaragonite
Reference	8.041	23.086	34.129	2281.9	409.965	2007.341	1798.117	196.978	4.76	3.115
	0.067	0.603	0.741	6.80	73.383	38.944	61.612	24.859	0.596	0.392
RCP 2.6	7.983	21.437	35.056	2282.93	493.011	2044.255	1855.972	173.103	4.144	2.703
	0.119	1.273	0.125	6.57	158.004	53	81.439	32.771	0.781	0.501
RCP 4.5	7.809	22.701	34.455	2283.32	765.545	2122.447	1973.165	126.296	3.043	1.99
	0.075	0.919	0.132	18.53	158.892	27.476	38.887	15.755	0.378	0.244
RCP 6.0	7.719	22.896	34.91	2271.84	970.706	2144.537	2008.7	106.928	2.568	1.681
	0.095	0.937	0.211	3.03	257.68	33.169	43.845	17.716	0.423	0.274
>RCP 8.5	7.529	22.072	34.723	2277.62	1803.047	2218.975	2088.23	75.92	1.823	1.19
	0.234	1.212	0.742	20.50	1287.448	82.982	82.43	33.368	0.799	0.519

pH_T, temperature, salinity ($n = 336$), and total alkalinity (A_T, $n = 4$) are measured values. Seawater pCO₂, dissolved inorganic carbon (DIC), bicarbonate (HCO₃⁻), carbonate (CO₃²⁻), saturation states for calcite (Ωcalcite), and aragonite (Ωaragonite) are values calculated using the carbonate chemistry system analysis program CO2SYS [29]. Values are presented as mean ± S.D. RCP refers to the representative concentration pathway.

Temperature, salinity, and pH_T were measured using multisensors (WQ-22C, TOA-DKK, Japan) deployed simultaneously at each site for one week in June 2019 ($n = 336$, with measurements taken every 30 min). Each meter was calibrated to pH total scale with a seawater standard and certified reference material (oceanic carbon dioxide quality control; obtained from the Andrew G. Dickson laboratory (Scripps Institution of Oceanography)). Total alkalinity samples were collected at each site ($n = 4$), immediately filtered at 0.45 μm using disposable cellulose acetate filters (Dismic, Advantech, Japan), and stored at room temperature in the dark until measurement. Total alkalinity was measured using an auto-titrator (916 Ti-Touch, Metrohm, Switzerland). Carbonate chemistry was calculated using the carbonate chemistry system analysis program CO2SYS [29] by using the measured values of pH_T, temperature, salinity, and total alkalinity. Disassociation constants from [30], as adjusted by [31], KSO₄ [32], and total borate concentrations from [33] were used.

For nutrients, three water samples were collected from each site (using 125 mL Nalgene polycarbonate bottles; Thermo Scientific, USA), and nutrients were analysed using a continuous segmented flow nutrients analyser (QuAAtro39 AutoAnalyzer, Seal Analytical) following standard protocols [34]. Redfield ratios were calculated as the ratio (in moles) of the carbon (C), silicate (Si), and nitrogen (N) to that of the phosphate (P). Carbon values were based on dissolved inorganic carbon measurements.

2.2. Field Survey

Percentage cover of *B. biddulphiana* was assessed using haphazardly distributed photoquadrats (50 × 50 cm, $n = 20$ –25 per site) on 17 April 2019 at a 5–7 m depth. In order to estimate the mean percentage cover, each photoquadrat was analysed using ImageJ [35] by overlaying 64 points on a grid, and recording the presence or absence of *B. biddulphiana* at each point.

Between 2017–2019, any observations of fish feeding on or interacting with the diatom mat were noted and when possible, the fish species feeding behaviour was qualitatively recorded by video (TG-5, Olympus, Japan).

2.3. Photophysiology and Production

A layer of *B. biddulphiana* (collected from their respective sites by hand in May 2019 from a depth of 5–7 m) was attached to 25 mm GFF filters (Whatmann, Pittsburgh, PA, USA) by briefly using a vacuum pump and filter holder in order to achieve a relatively homogenous and flat surface of diatoms. Three diatom-covered filters were prepared for each site and held in filtered seawater for 30 min for dark acclimation. The maximal quantum yield of electron transport yield (Fv/Fm), maximum light utilisation efficiency (α), and maximum absolute electron transport rate (ETR_{max}) were measured for

each diatom-covered filter using a Junior-PAM (Walz, Germany). The settings used for the PAM were measuring intensity (6), gain (1), saturation intensity (10), and signal width (0.8).

Diatom net oxygen production and respiration were measured in sealed 45 mL glass containers using four fibre-optic oxygen sensors (Firesting Pyroscience, Aachen, Germany) under light and dark conditions, respectively. Measurements were carried out over a 10 min period with O₂ measurements being carried out continuously, with a 30 min period in between light and dark measurements. The assumption was made that respiration rate in the light was at a similar rate to the rate in the dark. Diatoms were placed in filtered seawater (0.45 µm cellulose acetate filter), which was set to the appropriate pH/CO₂ via the bubbling of CO₂. Measurements were always carried out with one blank container to account for microbial respiration. Diatom biomass was standardised using Chlorophyll *a*, which was extracted with DMF (*N,N'*-dimethylformamide). After storage for one day in the dark at −20 °C, extinction coefficients were measured at three wavelengths (663.8, 646.8, and 750 nm), according to [36]. Analysis of the net oxygen production and respiration was performed using the 'RespR' package in R [37].

2.4. Associated Fauna

Associated fauna was collected using a scuba diver operated airlift to dislodge and lift samples into a 400 µm mesh net for later analysis. Collections were carried out at four plots (25 cm diameter circular quadrat) in the reference and RCP 6.0 sites during May 2016. The aim of sampling the associated fauna was to assess whether the diatom mat in the elevated *p*CO₂ conditions supported a similar faunal community relative to a representative equivalent in the reference *p*CO₂ (turf algae). Subsequently, random stratified sampling was used with turf algae being sampled in the reference *p*CO₂ site, and diatoms in the elevated *p*CO₂ site. Samples were fixed in 70% ethanol prior to sorting and identification. Samples were examined under a dissecting microscope, and organisms were separated from the turf/diatom. Fauna were identified to the highest taxonomic resolution possible, and abundance counted.

2.5. Statistical Analysis

All statistical analysis was performed in R (v 3.6.0) [38]. For abundance, the data did not conform to normality (QQ) or homogeneity of variance (Bartlett), and so a non-parametric (Kruskal–Wallis) test was used for assessing differences. For measurements of photophysiology, productivity, and faunal species richness, all data conformed to both normality (QQ) and homogeneity of variance (Bartlett). For PERMANOVA, the data conformed to the test for multivariate homogeneity of group dispersion, assessed used 'betadisper' [39].

3. Results and Discussion

The marine centric diatom *Biddulphia biddulphiana* (Figure 1A) is widespread, with records off North and South America, Western Europe, Australasia [40], and now Japan. It is often planktonic [41], but can use extracellular polymeric substances [42] to attach to benthic substrata. We found that in high CO₂ conditions it consistently forms mats that are up to several centimetres thick (Figure 1B,C). Monitoring along a natural carbon dioxide gradient off Shikine Island over the past five years (2015–2019) has shown that in areas with high CO₂, *B. biddulphiana* mats begin to appear in March–April, reaching their peak in June at depths of 6–8 m below Chart Datum (Figure 2C), and that each year, these mats last until the end of the summer (~late August–September) before being removed by strong wave action during typhoons. A similar bloom of *B. biddulphiana* was reported in tropical coral reefs in Mexico (within the Gulf of California), which formed turf-like mats that covered nearby corals [43].

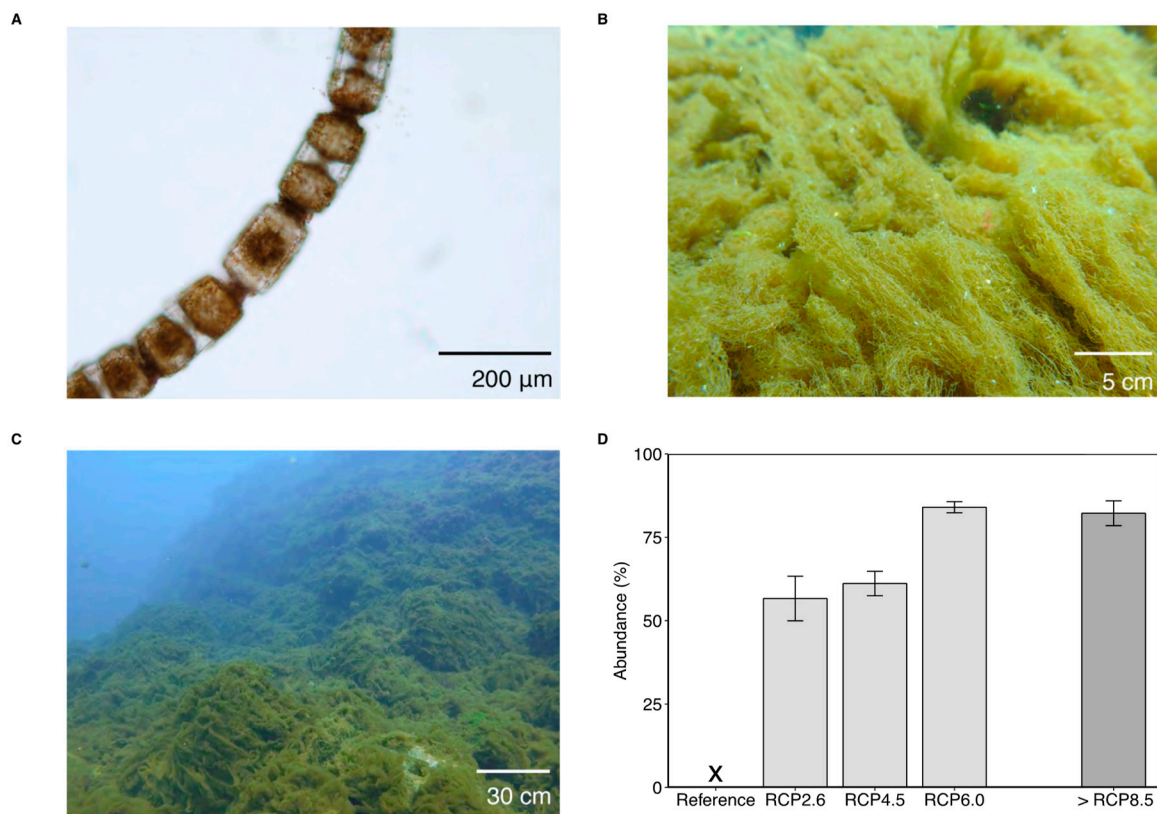


Figure 1. (A) Chain-forming *B. biddulphiana* diatoms, (B,C) these diatoms formed a turf-like mat at our RCP 6.0 sites. (D) Percentage cover of *B. biddulphiana*. NOTE: (i) The 'X' in panel (D) highlights that the survey was carried out, but zero percentage cover was observed. (ii) The >RCP 8.5 column is shaded and separated to highlight as it does not represent an end-of-the-century projection. Error bars are standard errors.

Benthic diatom mats were never seen by divers during hundreds of surveys at a depth of 0–10 m from 2015–2019 in reference $p\text{CO}_2$ conditions. Every year in this five-year monitoring period their abundance greatly increased with increasing $p\text{CO}_2$ (ANOVA: $F_{4,114} = 113.5$, $p < 0.001$; Figure 1D). Meta-barcoding of biofilms from a previous study revealed that *B. biddulphiana* were present in reference conditions, but not at high enough abundances for colonies to be visible with the naked eye [44] (May–June 2017, 6–8 m depth). In areas enriched with $p\text{CO}_2$, *B. biddulphiana* formed turf-like algal mats (1–10 cm in length, averaging approximately 5 cm in height), which dominated the seabed community (Figure 1). By reaching such a large biomass, and completely covering the seabed, the diatom mat provided a habitat for associated benthos and replaced the canopy forming macroalgae and scleractinian corals that dominated the reference CO_2 areas [22]. This suggests that the diatoms benefit from additional dissolved inorganic carbon in the water column and that this allows them to become the main habitat-forming species. Similar boosts in the abundance of diatoms due to elevated CO_2 have been shown previously [7,24,25], although this is the first study to show such a large biomass, with previous studies focussing on the microphytobenthos or phytoplankton.

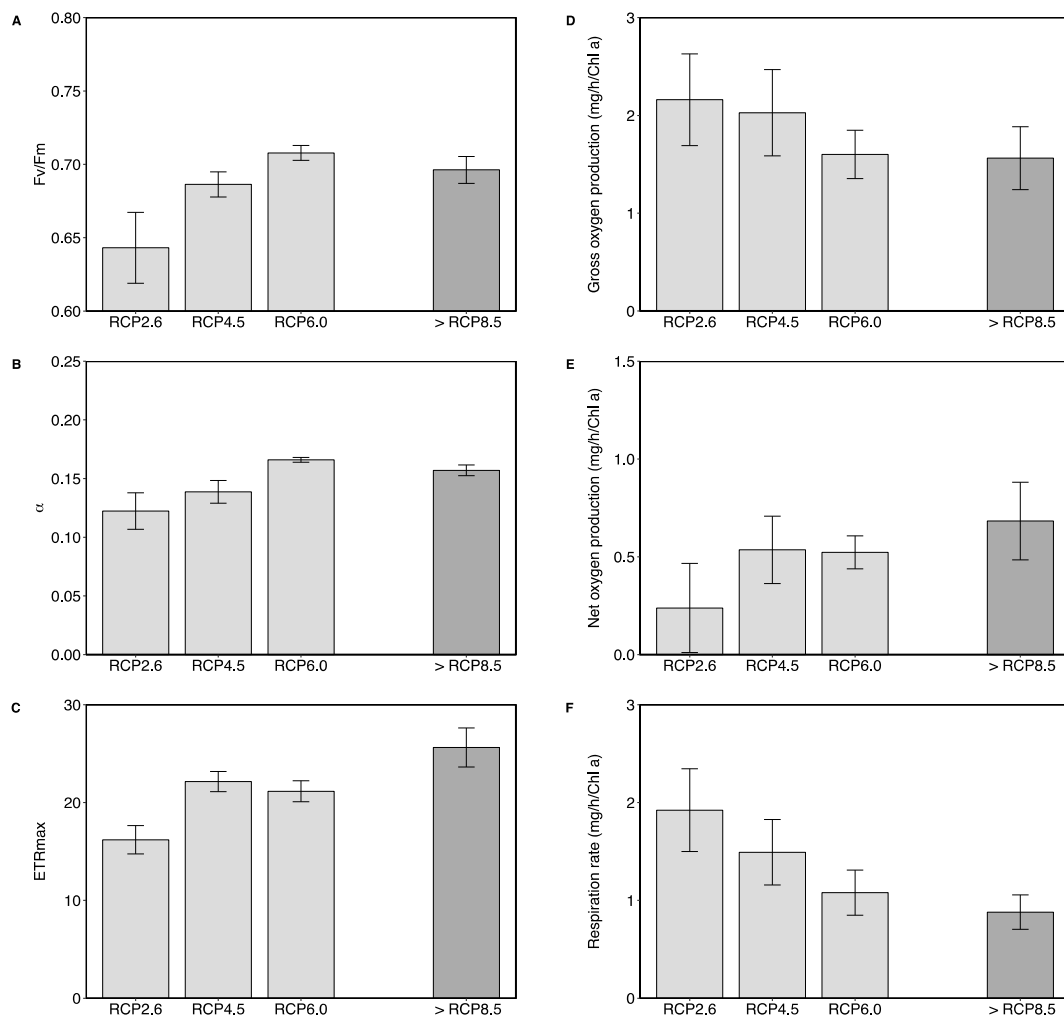


Figure 2. Photophysiology (A–C), and oxygen production and respiration (D–F) of the diatom *B. bidulphiana* under RCP 2.6, RCP 4.5, RCP 6.0, and >RCP 8.5 conditions. (A) Maximum quantum yield, Fv/Fm; (B) maximum light utilisation efficiency, α ; and (C) maximum absolute electron transport rate, ETRmax. (D) Gross oxygen production; (E) net oxygen production; and (F) respiration rate. NOTE: (i) Panel (A) scale starts from 0.6; and (ii) the >RCP 8.5 column is shaded and separated to highlight as it does not represent an end-of-the-century projection. Error bars are standard error.

Diatoms use silicic acid to form their silica frustules. The formation of this silica frustule is a requirement for diatom growth, leading to a strong requirement on silicic acid for growth. In addition, this biogenic silica plays a key role in proton-buffering, benefitting the diatom by facilitating the enzymatic conversion of bicarbonate into CO₂ [45]. Based on the Redfield–Brzezinski ratio of 106 (C):15 (Si):16 (N):1 (P) [46], which highlight the typical macronutrient requirements for diatoms, the growth of the diatoms in our site will have been mostly limited by N, and then by P, with Si levels non-limiting across all sites (Table 2 and Figure S1). Since the Redfield–Brzezinski ratio represents a canonical ratio of macronutrient uptake, it is probable that *B. bidulphiana* will have species-specific requirements (depending on its K_s , or the half-saturation constant), which could differ from the Redfield–Brzezinski ratio. Studies have not previously established the nutrient uptake kinetic constants for *B. bidulphiana*, highlighting the need for further research. Both nitrate and silicate are considered to be required in broadly equimolar amounts for many diatom species [47], and previous studies have found that the nitrate uptake kinetic constants (K_s) for *Biddulphia aurita* [48] are 2.12 ± 0.33 SE μM (strain STX-88 at 25 °C) and 3.19 ± 0.52 SE μM (strain B1 at 25 °C), and that for *Biddulphia sinensis* [49] is 0.74 ± 0.47 SE μM . Constants for *B. bidulphiana* in a similar range would therefore also suggest that nitrate concentrations

at our reference sites ($2.58 \mu\text{M NO}_3^- \pm 0.22 \text{ SD}$, $n = 3$) and elevated $p\text{CO}_2$ sites ($2.78 \mu\text{M NO}_3^- \pm 0.04 \text{ SD}$, $n = 3$) remain limited across all sites. As well as influencing growth and cell maintenance, it is thought that above a threshold of $2 \mu\text{M}$, SiO_4 diatoms can become dominant within phytoplankton communities [50]. Silicate concentrations were replete at our reference sites ($4.62 \mu\text{M SiO}_4 \pm 0.61 \text{ SD}$, $n = 3$) and elevated $p\text{CO}_2$ sites ($7.79 \mu\text{M SiO}_4 \pm 0.08 \text{ SD}$, $n = 3$) in the RCP 6.0 conditions), so a lack of silicate likely does not explain the lack of benthic diatom blooms at the reference site and surrounding area. Clearly, diatom community responses will not only be dictated by direct physiological responses to CO_2 and macronutrients [5]; they will be indirectly affected by acidification-driven impacts on grazers. Given the high grazing pressure within our reference $p\text{CO}_2$ site [22,51], predominantly associated with both herbivorous fish and sea urchins, it is possible that *B. biddulphiana* is being excluded. Our results strongly indicate that CO_2 enrichment stimulates diatom blooms and when combined with reductions in grazing pressure, allows them to become competitively dominant.

Table 2. Nutrient ratios (C:Si:N:P) of the reference $p\text{CO}_2$, RCP 2.6, RCP 4.5, RCP 6.0, and >RCP 8.5 conditions as well as the established Redfield–Brzezinski ratio for comparison.

Site	C	Si	N	P
Reference	9050	21	13	1
RCP 2.6	10,564	39	15	1
RCP 4.5	10,157	37	14	1
RCP 6.0	11,049	40	15	1
>RCP 8.5	11,469	128	12	1
Redfield–Brzezinski	106	15	16	1

C: carbon, Si: Silicate, N: Nitrogen, P: Phosphorus.

Marine diatoms are dominant marine primary producers [1] and have adapted to modern-day levels of CO_2 by operating a carbon concentrating mechanism (CCM), which allows them to elevate the concentration of CO_2 at the site of fixation by RubisCO [6]. When levels of seawater CO_2 increase, this can stimulate diatom growth through increased photosynthesis and lower energy use through downregulation of their CCMs [52,53]. In our study, enriched CO_2 resulted in significant increases in photosynthetic efficiency, in terms of the maximum quantum yield (F_v/F_m : $F_{3,8} = 4.17$, $p < 0.05$; Figure 2A), maximum light utilisation efficiency (α : $F_{3,8} = 4.18$, $p < 0.05$; Figure 2B) as well as maximum absolute electron transport rate (ETRmax: $F_{3,8} = 7.34$, $p < 0.05$; Figure 2C). Similar increases in the photosynthetic capacity of diatoms due to elevated CO_2 have been previously reported [54–56]. When measuring oxygen production, the gross oxygen production did not show any significant differences between the different sites ($F_{3,8} = 0.65$, $p = 0.62$; Figure 2D). Net oxygen production tended to increase with rising CO_2 (non-significantly, $F_{3,8} = 1.08$, $p = 0.41$; Figure 2E), and this appeared to be driven by a tendency for the respiration rate to decrease under elevated levels of $p\text{CO}_2$ (non-significantly, $F_{3,8} = 2.28$, $p = 0.16$; Figure 2F). Decreases in respiratory metabolism may synergise with the increased rate of C uptake due to increased photosynthesis, promote increased growth rates, and explain the greatly boosted abundance in our site with increasing $p\text{CO}_2$ levels. Although species-specific responses are likely for diatoms, some generalisations have been suggested, for example, diatoms with lower CCM efficiencies are more likely to show a pronounced response [57], and larger centric diatoms are more likely to profit relative to smaller species [11,12]. This body of work aligns with our novel observations of the effects of ocean acidification on *B. biddulphiana*.

Ocean acidification is expected to simplify communities as stress-intolerant species are lost, and opportunistic species attain competitive dominance [22,58,59]. From a previous study at the site, in reference conditions, a rocky reef habitat had a mixture of both canopy-forming fleshy macroalgae and zooxanthellate scleractinian corals, providing high levels of biodiversity and structural complexity [22]. This shifted to a diatom dominated algal turf community and so we wanted to assess how much associated biodiversity there was in the diatom-based benthic habitat when compared to the reference conditions. The expectation, based on other studies, was that by benefitting the weed-like growth of

just one algal species, this would reduce biodiversity and decrease ecosystem function, secondary productivity, and stability [59–61]. The mobile invertebrate communities that were supported by the diatom mat significantly differed from the communities found in seaweed habitats at reference levels of $p\text{CO}_2$ (PERMANOVA: $F_{1,7} = 6.59$, $p < 0.05$; Figure 3A and Figure S2). They had lower species richness, although this was not statistically significant at our level of sample replication ($F_{1,6} = 2.47$, $p = 0.17$; Figure 3B). Several taxa were absent in the elevated $p\text{CO}_2$ diatom mat (Figure S2), notably the calcified Decapoda and Mysida (Crustacea), Echinacea (Echinodermata), and Lucinoida (Bivalvia). Tanaids, which are less calcified, became the most abundant taxon comprising on average ~50% of individuals in elevated $p\text{CO}_2$ and only ~10% in the reference $p\text{CO}_2$ turf algae (Figure S2), suggesting competitive release (i.e., a decrease in their predation rates and/or increased availability of suitable habitat) [58,62].

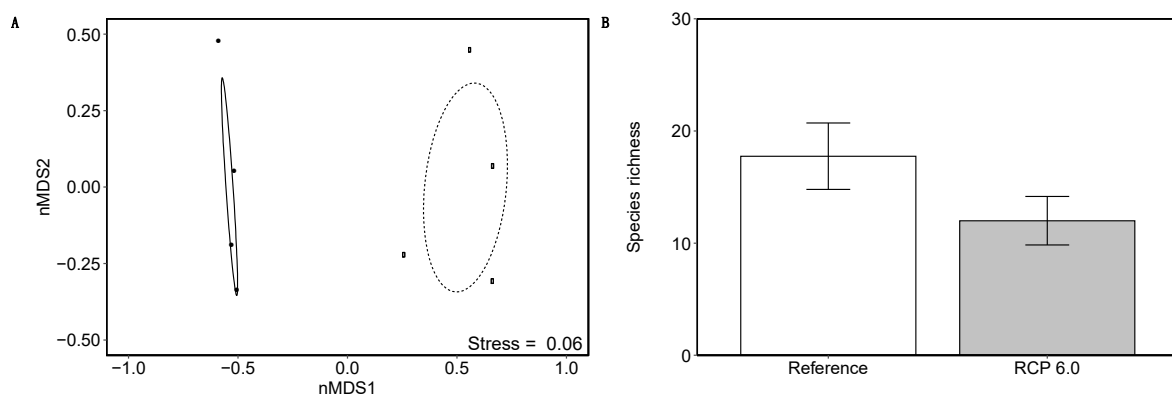


Figure 3. (A) nMDS mobile invertebrates in the reference $p\text{CO}_2$ turf-algae (dashed line, open circle) and elevated $p\text{CO}_2$ RCP 6.0 diatom mat (solid line, closed circle). (B) Species richness of the reference $p\text{CO}_2$ turf-algae (open) and elevated $p\text{CO}_2$ RCP 6.0 diatom mat (grey). Error bars are the standard error.

Diatoms form the basis of many food-webs, meaning that changes in their growth and/or abundance will have important ramifications for the trophic transfer of energy. In our study sites, the dominant grazers, in both the reference and elevated $p\text{CO}_2$ conditions, were herbivorous fish (personal observations). Despite herbivorous fishes being present, they did not graze down the boosted biomass of the turf-like diatoms (also see [61]). Only two fish species were seen consuming *B. biddulphiana*, based on ~120 h of in situ SCUBA diving observations, and these only ingested the diatom mat when consuming the invertebrate prey contained within. These were the benthophagous filter-feeding *Cheilodactylus zonatus* (Cuvier, 1830), which uses gill-rakers to capture small invertebrate prey ([63]; and see Figure 4 and Video S1) and the piscivorous and macroinvertebrate *Pseudocaranx dentex* (Bloch and Schneider, 1801), which used ram filtering and suction-feeding on *B. biddulphiana* to consume its prey ([64]; and see Video S2).

Carbon dioxide seeps are open systems that allow recruitment from outside, so while these systems are useful in showing which marine organisms are resilient today, it does not show the potential role that genetic adaptation will have over the coming years [22,60,65]. Regardless, the results of this study can provide important insights into how marine ecosystems could be altered in the near future. Increasing CO_2 levels were accompanied by a shift from diverse benthic communities of corals and macroalgae to a diatom turf community. Similar general patterns are seen at CO_2 seeps in tropical, sub-tropical, and temperate coastal systems with algal dominance, habitat degradation, and loss of biodiversity in acidified areas [66]. Diatom and turf algal blooms have been observed at other CO_2 seeps, for example, at the temperate White Island CO_2 seep in New Zealand where turf algae outcompete kelp [61]. Communities composed of simplified, opportunistic species have less ecological stability [67] since they can typically be succeeded by other competitively dominant species [68]. For a simple early successional community to maintain dominance suggests competitive exclusion and/or feedback loops that lock the system into a simplified state [68]. Overall, such shifts are likely to mean

that the coastal food-web structure and ecosystem function will become homogenised, simplified, and more strongly affected by seasonal algal blooms.

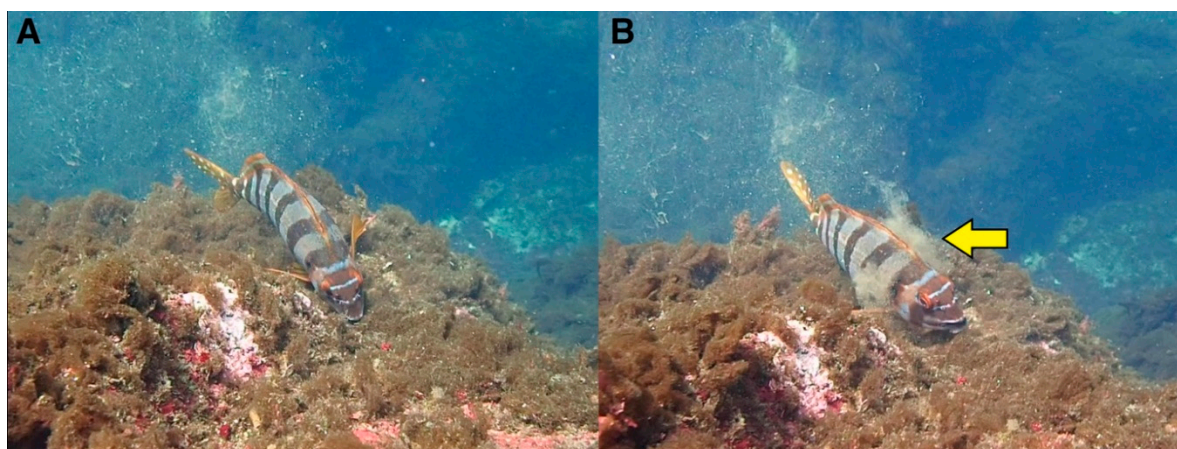


Figure 4. (A) The benthophagous filter-feeding *Cheilodactylus zonatus* (Cuvier, 1830) that uses gill-raking to capture small invertebrate prey from the diatom mat. (B) The yellow arrow indicates the remaining diatom being pushed through the gills (see Video S1 for a video of this feeding approach).

In conclusion, the seabed habitat analysed here showed significant changes resulting from CO₂ enrichment. Elevated levels of CO₂ stimulated the growth and photophysiology of a large chain-forming species of diatom, enabling it to become the dominant benthic habitat-forming species. This thick turf-like algal bloom was capable of supporting an abundant mobile faunal community, although the supported community differed from a typical seaweed community found in the reference pCO₂ conditions. Such ecological shifts will have important impacts on food web structure and ecosystem functioning.

Supplementary Materials: The following are available online at <http://www.mdpi.com/1424-2818/11/12/242/s1>. Figure S1: Nutrient concentrations (A–D) of the reference pCO₂, RCP 2.6, RCP 4.5, RCP 6.0, and >RCP 8.5 conditions. (A) Nitrite (NO₂), (B) Nitrate (NO₃⁻), (C) Phosphate (PO₄), and (D) Silicate (SiO₄). NOTE: The >RCP 8.5 column is shaded and separated to highlight as it does not represent an end-of-the-century projection. Error bars are the standard error; Figure S2: Abundance (individuals per m²) of the mobile invertebrate fauna found in the reference pCO₂ macroalgal turf (white filled) and elevated pCO₂ RCP 6.0 diatom mat (grey filled). Mobile invertebrate fauna are divided at the taxonomic order level, with broader taxonomic phylum groupings indicated. NOTE: Abundance is displayed using log scale. Error bars are the standard error. Video S1: Feeding behaviour of the benthophagous filter-feeding *Cheilodactylus zonatus*, which uses gill-raking to capture small invertebrate prey from the diatom mat; Video S2: Feeding behaviour of the piscivorous and macroinvertebrate *Pseudocaranx dentex*, which employs ram filtering and suction-feeding on *B. biddulphiana* to consume its prey.

Author Contributions: Conceptualisation, B.P.H.; Methodology, B.P.H.; Validation, B.P.H. and S.A.; Formal Analysis, B.P.H.; Investigation, B.P.H., S.A., K.K., and S.W.; Resources, B.P.H., S.A., K.K., and S.W.; Data Curation, B.H.; Writing—Original Draft Preparation, B.P.H.; Writing—Review & Editing, B.P.H., S.A., K.K., S.W., and J.M.H.-S.; Visualisation, B.P.H.; Supervision, B.P.H. and J.M.H.-S.; Project Administration, B.P.H.; Funding Acquisition, B.P.H., S.A., K.K., S.W., and J.M.H.-S.

Funding: This work was partially supported by Japan Society for the Promotion of Science (JSPS) KAKENHI grant number 17K17622, and the Ministry of Environment, Government of Japan (Suishinhi: 4RF-1701).

Acknowledgments: We thank Yasutaka Tsuchiya and the technical staff at the Shimoda Marine Research Centre, University of Tsukuba for their field assistance. This project contributes towards the ‘International Education and Research Laboratory Program’, University of Tsukuba. We acknowledge funding support from Japan Society for the Promotion of Science (JSPS) KAKENHI (grant number 17K17622), and the Ministry of Environment, Government of Japan (Suishinhi: 4RF-1701).

Conflicts of Interest: The authors declare no conflict of interest.

References

1. Nelson, D.M.; Tréguer, P.; Brzezinski, M.A.; Leynaert, A.; Quéguiner, B. Production and dissolution of biogenic silica in the ocean: Revised global estimates, comparison with regional data and relationship to biogenic sedimentation. *Glob. Biogeochem. Cycles* **1995**, *9*, 359–372. [[CrossRef](#)]
2. Harvey, B.P.; Gwynn-Jones, D.; Moore, P.J. Meta-analysis reveals complex marine biological responses to the interactive effects of ocean acidification and warming. *Ecol. Evol.* **2013**, *3*, 1016–1030. [[CrossRef](#)] [[PubMed](#)]
3. Gao, K.; Beardall, J.; Häder, D.-P.; Hall-Spencer, J.M.; Gao, G.; Hutchins, D.A. Effects of ocean acidification on marine photosynthetic organisms Under the concurrent influences of warming, UV radiation, and deoxygenation. *Front. Mar. Sci.* **2019**, *6*, 322. [[CrossRef](#)]
4. Brandenburg, K.M.; Velthuis, M.; Van de Waal, D.B. Meta-analysis reveals enhanced growth of marine harmful algae from temperate regions with warming and elevated CO₂ levels. *Glob. Chang. Biol.* **2019**, *25*, 2607–2618. [[CrossRef](#)]
5. Bach, L.T.; Taucher, J. CO₂ effects on diatoms: A synthesis of more than a decade of ocean acidification experiments with natural communities. *Ocean Sci.* **2019**, *15*, 1159–1175. [[CrossRef](#)]
6. Reinfelder, J.R. Carbon concentrating mechanisms in eukaryotic marine phytoplankton. *Annu. Rev. Mar. Sci.* **2011**, *3*, 291–315. [[CrossRef](#)]
7. Bach, L.T.; Hernández-Hernández, N.; Taucher, J.; Spisla, C.; Sforna, C.; Riebesell, U.; Aristegui, J. Effects of elevated CO₂ on a natural diatom community in the subtropical NE Atlantic. *Front. Mar. Sci.* **2019**, *6*, 75. [[CrossRef](#)]
8. Macreadie, P.I.; Anton, A.; Raven, J.A.; Beaumont, N.; Connolly, R.M.; Friess, D.A.; Kelleway, J.J.; Kennedy, H.; Kuwae, T.; Lavery, P.S.; et al. The future of Blue Carbon science. *Nat. Commun.* **2019**, *10*, 3998. [[CrossRef](#)]
9. Sarthou, G.; Timmermans, K.R.; Blain, S.; Tréguer, P. Growth physiology and fate of diatoms in the ocean: A review. *Iron Resour. Ocean. Nutr. Adv. Glob. Environ. Simul.* **2005**, *53*, 25–42. [[CrossRef](#)]
10. Flynn, K.J.; Blackford, J.C.; Baird, M.E.; Raven, J.A.; Clark, D.R.; Beardall, J.; Brownlee, C.; Fabian, H.; Wheeler, G.L. Changes in pH at the exterior surface of plankton with ocean acidification. *Nat. Clim. Chang.* **2012**, *2*, 510–513. [[CrossRef](#)]
11. Tortell, P.D.; Payne, C.D.; Li, Y.; Trimborn, S.; Rost, B.; Smith, W.O.; Riesselman, C.; Dunbar, R.B.; Sedwick, P.; DiTullio, G.R. CO₂ sensitivity of Southern Ocean phytoplankton. *Geophys. Res. Lett.* **2008**, *35*. [[CrossRef](#)]
12. Feng, Y.; Hare, C.E.; Rose, J.M.; Handy, S.M.; DiTullio, G.R.; Lee, P.A.; Smith, W.O.; Peloquin, J.; Tozzi, S.; Sun, J.; et al. Interactive effects of iron, irradiance and CO₂ on Ross Sea phytoplankton. *Deep Sea Res. Part Oceanogr. Res. Pap.* **2010**, *57*, 368–383. [[CrossRef](#)]
13. Sommer, U.; Stibor, H.; Katechakis, A.; Sommer, F.; Hansen, T. Pelagic food web configurations at different levels of nutrient richness and their implications for the ratio fish production:primary production. *Hydrobiologia* **2002**, *484*, 11–20. [[CrossRef](#)]
14. Feng, Y.; Hare, C.E.; Leblanc, K.; Rose, J.M.; Zhang, Y.; DiTullio, G.R.; Lee, P.A.; Wilhelm, S.W.; Rowe, J.M.; Sun, J.; et al. Effects of increased pCO₂ and temperature on the North Atlantic spring bloom. I. The phytoplankton community and biogeochemical response. *Mar. Ecol. Prog. Ser.* **2009**, *388*, 13–25. [[CrossRef](#)]
15. Eggers, S.L.; Lewandowska, A.M.; Barcelos, E.; Ramos, J.; Blanco-Ameijeiras, S.; Gallo, F.; Matthiessen, B. Community composition has greater impact on the functioning of marine phytoplankton communities than ocean acidification. *Glob. Chang. Biol.* **2014**, *20*, 713–723. [[CrossRef](#)] [[PubMed](#)]
16. Taucher, J.; Bach, L.T.; Boxhammer, T.; Nauendorf, A.; Achterberg, E.P.; Algueró-Muñiz, M.; Aristegui, J.; Czerny, J.; Esposito, M.; Guan, W.; et al. Influence of ocean acidification and deep water upwelling on oligotrophic plankton communities in the subtropical North Atlantic: Insights from an in situ mesocosm study. *Front. Mar. Sci.* **2017**, *4*, 85. [[CrossRef](#)]
17. Bach, L.T.; Alvarez-Fernandez, S.; Hornick, T.; Stuhr, A.; Riebesell, U. Simulated ocean acidification reveals winners and losers in coastal phytoplankton. *PLoS ONE* **2017**, *12*, e0188198. [[CrossRef](#)] [[PubMed](#)]
18. Schulz, K.G.; Bach, L.T.; Bellerby, R.G.J.; Bermúdez, R.; Büdenbender, J.; Boxhammer, T.; Czerny, J.; Engel, A.; Ludwig, A.; Meyerhöfer, M.; et al. Phytoplankton blooms at increasing levels of atmospheric carbon dioxide: Experimental evidence for negative effects on prymnesiophytes and positive on small picoeukaryotes. *Front. Mar. Sci.* **2017**, *4*, 64. [[CrossRef](#)]

19. Calvo-Díaz, A.; Díaz-Pérez, L.; Suárez, L.Á.; Morán, X.A.G.; Teira, E.; Marañón, E. Decrease in the autotrophic-to-heterotrophic biomass ratio of picoplankton in oligotrophic marine waters due to bottle enclosure. *Appl. Environ. Microbiol.* **2011**, *77*, 5739. [[CrossRef](#)]
20. Riebesell, U.; Aberle-Malzahn, N.; Achterberg, E.P.; Algueró-Muñiz, M.; Alvarez-Fernandez, S.; Arístegui, J.; Bach, L.T.; Boersma, M.; Boxhammer, T.; Guan, W.; et al. Toxic algal bloom induced by ocean acidification disrupts the pelagic food web. *Nat. Clim. Chang.* **2018**, *8*, 1082–1086. [[CrossRef](#)]
21. Fabricius, K.E.; Langdon, C.; Uthicke, S.; Humphrey, C.; Noonan, S.; De'ath, G.; Okazaki, R.; Muehllehner, N.; Glas, M.S.; Lough, J.M. Losers and winners in coral reefs acclimatized to elevated carbon dioxide concentrations. *Nat. Clim. Chang.* **2011**, *1*, 165–169. [[CrossRef](#)]
22. Agostini, S.; Harvey, B.P.; Wada, S.; Kon, K.; Milazzo, M.; Inaba, K.; Hall-Spencer, J.M. Ocean acidification drives community shifts towards simplified non-calcified habitats in a subtropical-temperate transition zone. *Sci. Rep.* **2018**, *8*, 11354. [[CrossRef](#)]
23. Hall-Spencer, J.M.; Rodolfo-Metalpa, R.; Martin, S.; Ransome, E.; Fine, M.; Turner, S.M.; Rowley, S.J.; Tedesco, D.; Buia, M.-C. Volcanic carbon dioxide vents show ecosystem effects of ocean acidification. *Nature* **2008**, *454*, 96–99. [[CrossRef](#)]
24. Johnson, V.R.; Brownlee, C.; Rickaby, R.E.M.; Graziano, M.; Milazzo, M.; Hall-Spencer, J.M. Responses of marine benthic microalgae to elevated CO₂. *Mar. Biol.* **2011**, *160*, 1813–1824. [[CrossRef](#)]
25. Johnson, R.V.; Brownlee, C.; Milazzo, M.; Hall-Spencer, M.J. Marine microphytobenthic assemblage shift along a natural shallow-water CO₂ gradient subjected to multiple environmental stressors. *J. Mar. Sci. Eng.* **2015**, *3*, 1425–1447. [[CrossRef](#)]
26. Harvey, B.P.; Agostini, S.; Wada, S.; Inaba, K.; Hall-Spencer, J.M. Dissolution: the Achilles' heel of the triton shell in an acidifying ocean. *Front. Mar. Sci.* **2018**, *5*, 371. [[CrossRef](#)]
27. IPCC. *Climate Change 2013—The Physical Science Basis: Working Group I Contribution to the Fifth Assessment Report of the IPCC*; Cambridge University Press: Cambridge, UK, 2013; p. 1535.
28. Agostini, S.; Wada, S.; Kon, K.; Omori, A.; Kohtsuka, H.; Fujimura, H.; Tsuchiya, Y.; Sato, T.; Shinagawa, H.; Yamada, Y.; et al. Geochemistry of two shallow CO₂ seeps in Shikine Island (Japan) and their potential for ocean acidification research. *Reg. Stud. Mar. Sci.* **2015**, *2*, 45–53. [[CrossRef](#)]
29. Pierrot, D.; Lewis, E.; Wallace, D.W.R. *MS Excel Program Developed for CO₂ System Calculations*, ORNL/CDIAC-105; Carbon Dioxide Information Analysis Center, Oak Ridge National Laboratory, US Department of Energy: Oak Ridge, TN, USA, 2006.
30. Mehrbach, C.; Culberson, C.H.; Hawley, J.E.; Pytkowicz, R.M. Measurement of the apparent dissociation constants of carbonic acid in seawater at atmospheric pressure. *Limnol. Oceanogr.* **1973**, *18*, 897–907. [[CrossRef](#)]
31. Dickson, A.G.; Millero, F.J. A comparison of the equilibrium constants for the dissociation of carbonic acid in seawater media. *Deep Sea Res. Part Oceanogr. Res. Pap.* **1987**, *34*, 1733–1743. [[CrossRef](#)]
32. Dickson, A.G. Thermodynamics of the dissociation of boric acid in potassium chloride solutions from 273.15 to 318.15 K. *J. Chem. Eng. Data* **1990**, *35*, 253–257. [[CrossRef](#)]
33. Uppström, L.R. The boron/chlorinity ratio of deep-sea water from the Pacific Ocean. *Deep Sea Res. Oceanogr. Abstr.* **1974**, *21*, 161–162. [[CrossRef](#)]
34. Hansen, H.; Koroleff, F. Determination of Nutrients. In *Methods of Seawater Analysis*; Grasshoff, K., Kremling, K., Ehrhardt, M., Eds.; John Wiley & Sons Ltd.: Hoboken, NJ, USA, 2007; pp. 159–228.
35. Abràmoff, M.D.; Magalhães, P.J.; Ram, S.J. Image processing with ImageJ. *Biophotonics Int.* **2004**, *11*, 36–42.
36. Porra, R.; Thompson, W.; Kriedemann, P. Determination of accurate extinction coefficients and simultaneous equations for assaying chlorophylls a and b extracted with four different solvents: Verification of the concentration of chlorophyll standards by atomic absorption spectroscopy. *Biochim. Biophys. Acta BBA Bioenerg.* **1989**, *975*, 384–394. [[CrossRef](#)]
37. Harianto, J.; Carey, N.; Byrne, M. RespR—An R package for the manipulation and analysis of respirometry data. *Methods Ecol. Evol.* **2019**, *10*, 912–920. [[CrossRef](#)]
38. Team, R.C. R: A Language and Environment for Statistical Computing. *Dev. Core* **2019**, 201. Available online: <https://www.r-project.org/> (accessed on 10 December 2019).
39. Oksanen, J.; Blanchet, F.G.; Friendly, M.; Kindt, R.; Legendre, P.; McGlenn, D.; Minchin, P.R.; O'Hara, R.B.; Simpson, G.L.; Solymos, P.; et al. Vegan: Community Ecology Package (R Package Version 2.5–5). 2019. Available online: <https://rdrr.io/cran/vegan/> (accessed on 10 October 2019).

40. Kociolek, J.P.; Coste, M.; Ector, L.; Liu, Y.; Kulikovskiy, M.; Lundholm, N.; Ludwig, T.; Potapova, M.; Rimet, F.; Sabbe, K.; et al. DiatomBase *Biddulphia Biddulphiana* (J.E.Smith) Boyer. 1900. Available online: <http://www.diatombase.org/aphia.php?p=taxdetails&id=162952> (accessed on 1 June 2018).
41. Round, F.E.; Crawford, R.M.; Mann, D.G. *Diatoms: Biology and Morphology of the Genera*; Cambridge University Press: Cambridge, UK, 1990; ISBN 978-0-521-36318-1.
42. Hoagland, K.D.; Rosowski, J.R.; Gretz, M.R.; Roemer, S.C. Diatom extracellular polymeric substances: Function, fine structure, chemistry, and physiology. *J. Phycol.* **1993**, *29*, 537–566. [[CrossRef](#)]
43. Galland, G.R.; Pennebaker, S.L. A benthic diatom bloom in the Gulf of California, Mexico. *BioInvasions Rec.* **2012**, *1*, 65–69. [[CrossRef](#)]
44. Allen, R.; Summerfield, T.C.; Harvey, B.P.; Agostini, S.; Rastrick, S.P.S.; Hall-Spencer, J.M.; Hoffmann, L.J. The effect of ocean acidification on biofilm community composition and early successional dynamics: A high-throughput sequencing study. Unpublished work, 2019.
45. Milligan, A.J.; Morel, F.M.M. A proton buffering role for silica in diatoms. *Science* **2002**, *297*, 1848–1850. [[CrossRef](#)]
46. Brzezinski, M.A. The Si:C:N ratio of marine diatoms: Interspecific variability and the effects of some environmental variables. *J. Phycol.* **1985**, *21*, 347–357. [[CrossRef](#)]
47. Flynn, K.J.; Martin-Jézéquel, V. Modelling Si–N-limited growth of diatoms. *J. Plankton Res.* **2000**, *22*, 447–472. [[CrossRef](#)]
48. Underhill, P.A. Nitrate uptake kinetics and clonal variability in the neritic diatom *Biddulphia aurita*. *J. Phycol.* **1977**, *13*, 170–176. [[CrossRef](#)]
49. Qasim, S.Z.; Bhattathiri, P.M.A.; Devassy, V.P. Growth kinetics and nutrient requirements of two tropical marine phytoplankters. *Mar. Biol.* **1973**, *21*, 299–304. [[CrossRef](#)]
50. Egge, J.; Aksnes, D. Silicate as regulating nutrient in phytoplankton competition. *Mar. Ecol. Prog. Ser.* **1992**, *83*, 281–289. [[CrossRef](#)]
51. Cattano, C.; Agostini, S.; Harvey, B.P.; Wada, S.; Quattrocchi, F.; Turco, G.; Inaba, K.; Hall-Spencer, J.M.; Milazzo, M. Consistent spatio-temporal changes in fish communities as a result of benthic habitat shifts under ocean acidification conditions. Unpublished work, 2019.
52. Hopkinson, B.M.; Dupont, C.L.; Allen, A.E.; Morel, F.M. Efficiency of the CO₂-concentrating mechanism of diatoms. *Proc. Natl. Acad. Sci. USA* **2011**, *108*, 3830–3837. [[CrossRef](#)]
53. Young, J.N.; Morel, F.M. Biological oceanography: The CO₂ switch in diatoms. *Nat. Clim. Chang.* **2015**, *5*, 722. [[CrossRef](#)]
54. Trimborn, S.; Wolf-Gladrow, D.; Richter, K.-U.; Rost, B. The effect of pCO₂ on carbon acquisition and intracellular assimilation in four marine diatoms. *J. Exp. Mar. Bio. Ecol.* **2009**, *376*, 26–36. [[CrossRef](#)]
55. Wu, Y.; Gao, K.; Riebesell, U. CO₂-induced seawater acidification affects physiological performance of the marine diatom *Phaeodactylum tricorutum*. *Biogeosciences* **2010**, *7*, 2915–2923. [[CrossRef](#)]
56. Yang, G.; Gao, K. Physiological responses of the marine diatom *Thalassiosira pseudonana* to increased pCO₂ and seawater acidity. *Mar. Environ. Res.* **2012**, *79*, 142–151. [[CrossRef](#)]
57. Shi, D.; Hong, H.; Su, X.; Liao, L.; Chang, S.; Lin, W. The physiological response of marine diatoms to ocean acidification: Differential roles of seawater pCO₂ and pH. *J. Phycol.* **2019**, *55*, 521–533. [[CrossRef](#)]
58. Kroeker, K.J.; Micheli, F.; Gambi, M.C.; Martz, T.R. Divergent ecosystem responses within a benthic marine community to ocean acidification. *Proc. Natl. Acad. Sci. USA* **2011**, *108*, 14515–14520. [[CrossRef](#)]
59. Vizzini, S.; Martínez-Crego, B.; Andolina, C.; Massa-Gallucci, A.; Connell, S.D.; Gambi, M.C. Ocean acidification as a driver of community simplification via the collapse of higher-order and rise of lower-order consumers. *Sci. Rep.* **2017**, *7*, 4018. [[CrossRef](#)]
60. Harvey, B.P.; Al-Janabi, B.; Broszeit, S.; Cioffi, R.; Kumar, A.; Aranguren-Gassis, M.; Bailey, A.; Green, L.; Gsottbauer, C.M.; Hall, E.F.; et al. Evolution of marine organisms under climate change at different levels of biological organisation. *Water* **2014**, *6*, 3545–3574. [[CrossRef](#)]
61. Connell, S.D.; Doubleday, Z.A.; Foster, N.R.; Hamlyn, S.B.; Harley, C.D.G.; Helmuth, B.; Kelaher, B.P.; Nagelkerken, I.; Rodgers, K.L.; Sarà, G.; et al. The duality of ocean acidification as a resource and a stressor. *Ecology* **2018**, *99*, 1005–1010. [[CrossRef](#)] [[PubMed](#)]
62. Micheli, F.; Cottingham, K.L.; Bascompte, J.; Bjørnstad, O.N.; Eckert, G.L.; Fischer, J.M.; Keitt, T.H.; Kendall, B.E.; Klug, J.L.; Rusak, J.A. The dual nature of community variability. *Oikos* **1999**, *85*, 161–169. [[CrossRef](#)]

63. Matsumoto, K.; Kohda, M. Differences in gill raker morphology between two local populations of a benthophagous filter-feeding fish, *Goniistius zonatus* (Cheilodactylidae). *Ichthyol. Res.* **2001**, *48*, 269–273. [[CrossRef](#)]
64. Sazima, I. Field evidence for suspension feeding in *Pseudocaranx dentex*, with comments on ram filtering in other jacks (Carangidae). *Environ. Biol. Fishes* **1998**, *53*, 225–229. [[CrossRef](#)]
65. Sunday, J.M.; Calosi, P.; Dupont, S.; Munday, P.L.; Stillman, J.H.; Reusch, T.B.H. Evolution in an acidifying ocean. *Trends Ecol. Evol.* **2014**, *29*, 117–125. [[CrossRef](#)]
66. Hall-Spencer, J.M.; Harvey, B.P. Ocean acidification impacts on coastal ecosystem services due to habitat degradation. *Emerg. Top. Life Sci.* **2019**, *3*, 197–206.
67. Hooper, D.U.; Adair, E.C.; Cardinale, B.J.; Byrnes, J.E.K.; Hungate, B.A.; Matulich, K.L.; Gonzalez, A.; Duffy, J.E.; Gamfeldt, L.; O'Connor, M.I. A global synthesis reveals biodiversity loss as a major driver of ecosystem change. *Nature* **2012**, *486*, 105–108. [[CrossRef](#)]
68. Connell, J.H.; Slatyer, R.O. Mechanisms of succession in natural communities and their role in community stability and organization. *Am. Nat.* **1977**, *111*, 1119–1144. [[CrossRef](#)]



© 2019 by the authors. Licensee MDPI, Basel, Switzerland. This article is an open access article distributed under the terms and conditions of the Creative Commons Attribution (CC BY) license (<http://creativecommons.org/licenses/by/4.0/>).